Folding Dendrons: The Development of Solvent-, Temperature-, and Generation-Dependent Chiral Conformational Order in Intramolecularly Hydrogen-Bonded Dendrons

Janosch Recker, Dennis J. Tomcik, and Jon R. Parquette*

Contribution from the Department of Chemistry, The Ohio State University, Columbus, Ohio 43210

Received April 7, 2000

Abstract: The synthesis of intramolecularly hydrogen-bonded dendrons with stereogenic terminal groups derived from (1*S*,2*S*)-(+)-thiomicamine up to the third generation is described. Circular dichroism (CD) studies reveal that the equilibria interconverting two diastereomeric helical conformations (M and P helices) relating a pair of anthranilamide termini depends on solvent, temperature, and dendrimer generation. A conformational preference for M-type helicity along the periphery of the dendrons increased with increasing dendrimer generation and in poor solvents as observed by CD. Equilibration of these diastereomeric helical conformations is rapid at the first generation in all solvents and at all temperatures investigated; however, at the second generation the equilibrium begins to bias a single diastereomeric helical conformation along the periphery that becomes maximal at low temperatures and in poor solvents. At the third generation, the helical bias is intrinsically higher so that the conformational preference of the termini becomes much less sensitive to solvent and temperature, and the unfolding process becomes more difficult. We propose that nonbonded repulsive interactions that increase with generation and in poor solvents couple the motions and conformational preferences of each pair of terminal groups through their correlated rotations and contribute to the stability of the M helical conformation of the terminal groups. This represents the first example of well-defined asymmetric secondary structure occurring in a dendrimer system.

Introduction

Nature consistently relies on large macromolecules such as proteins to perform the many important chemical functions required for life. A minimization of free energy that is determined by the cooperative action of many noncovalent interactions drives a folding process in these large molecules to produce a specific 3-dimensional structure that is crucial for function.[1] The design of unnatural molecules that fold into predictable and well-defined conformations can provide insight into some of the interactions that control the folding of peptides into stable tertiary structures.[2] In particular, the conformation of chiral dendrimers has been of great interest because their highly branched structure creates a globular morphology that potentially mimics globular proteins.[3] The development of higher levels of self-organization in a chiral dendrimer would be expressed as asymmetric conformational order and should be observable using chiroptical methods.[4] Although numerous chiroptical studies of chiral dendrimers have been reported, these studies were unable to unambiguously ascertain the presence of a secondary structural fold and most suggested a lack of conformational order.[4,6−16] More importantly, an understanding of the nature of the conformational equilibrium present in these dendrimers has not been forthcoming. In this work, we report

(1) Creighton, T. E. *Proteins: Structures and Molecular Properties*, 2nd ed.; W. H. Freeman: New York, 1993.

(2) (a) Barron, A. E.; Zuckermann, R. N. *Curr. Opin. Chem. Biol.* **1999**, *3*(6), 681. (b) Kirshenbaum, K.; Zuckermann, R. N.; Dill, K. A. *Curr. Opin. Struct. Biol.* **1999**, *9*(*4*), 530. (c) Smith, M. D.; Fleet, G. W. J. *J. Pept. Sci*. **1999**, *5*(*10*), 425.

(3) (a) Fischer, M.; Vögtle, F. *Angew. Chem., Int. Ed.* **1999**; *38*, 885. (b) Smith, D. K.; Diederich, F. *Chem.−Eur. J.* **1998**, *4*(8), 1353.

(4) For some reviews of chiral dendrimers, see: (a) Seebach, D.; Rheiner, P. B.; Greiveldinger, G.; Butz, T.; Sellner, H. *Top. Curr. Chem.* **1998**, *197*, 125. (b) Peerlings, H. W. I.; Meijer, E. W. *Chem. Eur. J.* **1997**, *3*, 1563. (c) Thomas, C. W.; Tor, Y. *Chirality* **1998**, *10*, 53.

(5) For a discussion of the relationship of optical activity to conformation in linear polymers, see: (a) Farina, M. *Top. Stereochem.* **1987**, *17*1. (b) Pino, P.; Salvadori, P.; Chiellini, E.; Luisi, P. L. *Pure Appl. Chem.* **1968**, *16*(2−3), 469.

(6) (a) McElhanon, J. R.; McGrath, D. V. *J. Org. Chem.* **2000**, *65*(11), 3525. (b) McElhanon, J. R.; McGrath, D. V. *J. Am. Chem. Soc.* **1998**, *120*, 1647. (c) Junge, D. M.; McGrath, D. V. *Tetrahedron Lett.* **1998**, *39*, 1701. (d) McGrath, D. V.; Wu, M.-J.; Chaudhry, U. *Tetrahedron Lett.* **1996**, *37*, 6077. (e) McElhanon, J. R.; Wu, M.-J.; Escobar, M.; McGrath, D. V. *Macromolecules* **1996**, *29*, 8979. (f) Chang, H.-T.; Chen, C.-T.; Kondo, T.; Siuzdak, G.; Sharpless, K. B. *Angew. Chem., Int. Ed. Engl.* **1996**, *35*, 182. (g) Balasubramanian, R.; Rao, P.; Maitra, U. *Chem. Commun.* **1999**, (23), 2353.

(7) (a) Kress, J.; Rosner, A.; Hirsch, A. *Chem.−Eur. J.* **2000**, *6*, 247. (b) Chow, H.-F.; Mak, C. C. *J. Chem. Soc., Perkin Trans. 1* **1997**, 91. (c) Chow, H.-F.; Mak, C. C. *Pure Appl. Chem.* **1997**, *69*, 483. (d) Mak, C. C.; Chow, H.-F. *Chem. Commun.* **1996**, 1185. (e) Chow, H.-F.; Mak, C. C. *Tetrahedron Lett.* **1996**, *37*, 5935.

(8) (a) Lartigue, M.-L.; Caminade, A.-M.; Majoral, J. P. *Tetrahedron: Asymmetry* **1997**, *8*, 2697. (b) Issberner, J.; Boehme, M.; Grimme, S.; Nieger, M.; Paulus, W.; Vögtle, F. *Tetrahedron: Asymmetry* **1996**, *7*, 2223. (c) Issberner, J.; Bohme, M.; Grimme, S.; Nieger, M.; Paulus, W.; Vogtle, F. *Tetrahedron Asymmetry* **1996**, *7*, 7. (d) Newkome, G. R.; Lin, X.; Weis, C. D. *Tetrahedron: Asymmetry* **1991**, *2*, 957.

(9) (a) Jansen, J. F. G. A.; Peerlings, H. W. I.; de Brabander-Van den Berg, E. M. M.; Meijer, E. W. *Angew. Chem., Int. Ed. Engl.* **1995**, *34*, 1206. (b) Jansen, J.; de Brabander-Van den Berg, E. M. M.; Meijer, E. W. *Recl. Trav. Chim. Pays-Bas.* **1995**, *114*, 225.

(10) (a) Murer, P. K.; Lapierre, J. M.; Greiveldinger, G.; Seebach, D. *Helv. Chim. Acta* **1997**, *80*, 1648. (b) Murer, P.; Seebach, D. *Angew. Chem., Int. Ed. Engl.* **1995**, *34*, 2116.

(11) Murer, P.; Seebach, D. *Helv. Chim. Acta* **1998**, *81*, 603.

(12) (a) Seebach, D.; Lapierre, J. M.; Skobridis, K.; Greiveldinger, G. *Angew. Chem., Int. Ed. Engl.* **1994**, *33*, 440. (b) Seebach, D.; Lapierre, J. M.; Greiveldinger, G.; Skobridis, K. *Helv. Chim. Acta* **1994**, *77*, 1673. (c).

(13) Hu, Q.-S.; Pugh, V.; Sabat, M.; Pu, L. *J. Org. Chem.* **1999**, *64*, 4(20), 7528.

10.1021/ja001225c CCC: $19.00
Published on Web 10/04/2000

the first example of a dendron that develops chiral secondary structural order and describe how intramolecular hydrogen-bonding, noncovalent packing interactions, solvophobic compression, and dendrimer generation contribute to the stability of a particular helical conformation.

Chiroptical studies of chiral dendrimers commonly infer conformational information by comparing the chiroptical properties of several generations of dendrimers to that of the repeating chiral subunit[6−16] or of a suitable model compound.[6a−c] Any deviation of the dendrimer optical activity, normalized for the number of repeating chiral chromophores, and the optical activity of the chiral subunit are interpreted as a shift in the position of conformational equilibrium.[5] The majority of chiral dendrimers that have been described exhibit optical rotations or circular dichroisms that vary linearly with the number of repeating chiral chromophores, indicating that stable secondary structural order was not developing. For example, several reports demonstrated that dendrimers with fully chiral branches based on chiral polyaryl ether[6] or tartaric acid[7] subunits exhibited specific rotations linearly proportionate to the number of chiral chromophores. Dendrimers with stereogenic substituents at the surface also appear to exhibit chiroptical data that vary proportionately to the number of stereogenic termini.[8] In contrast to these observations, Meijer observed that poly(propyleneamine) dendrimers displaying amino acids on the periphery undergo a decrease in specific rotation with dendrimer generation.[9] However, this behavior could be attributed to the presence of a densely packed periphery that significantly reduced the conformational freedom of the chiral terminal groups creating a number of frozen conformations with pseudo-enantiomeric relationships. Seebach has also observed anomalous variations in chiroptical data with dendrimer generation in fully chiral dendrimers,[10] and recently, in a related dendrimer system, a variation in the sign and shape of the CD spectra with dendrimer generation was observed in acetonitrile but not in a good solvent such as dichloromethane.[11] However, the nature of the conformational equilibrium and the origin of the solvent effect could not be determined. Chiroptical studies of dendrimers constructed from a chiral central core also suggest that conformational asymmetry is unlikely to be present. For example, Seebach has shown that polyaryl ether dendrimers with a stereogenic core and achiral branches exhibit molar rotations that remain approximately constant with generation, indicating that chiral conformations were not contributing to the observed rotations.[12] Similarly, phenylacetylene dendrimers with a chiral 1,1′-bi-2-naphthol central core exhibited CD spectra that were invariant with generation, indicating the achiral dendrons were not adopting chiral conformations.[13] We and others have observed variations in molar rotation with generation in dendrimers containing chiral central cores that could be attributed to a generation-dependent perturbation in the conformational equilibrium of the central core rather than chiral conformational order.[14,15] Meijer reported that polyaryl ether dendrimers that were chiral based on the linkage of three constitutionally different dendritic wedges displayed no optical activity as a consequence of the conformational flexibility of the branches.[16] These seminal studies are consistent with recent evidence suggesting that, in the absence of attractive or repulsive secondary interactions between otherwise flexible dendritic subunits, most dendrimers are conformationally quite flexible especially at lower generations.[17] Consequently, conformationally flexible dendrimers do not adopt the well-defined supramolecular structure necessary to induce higher levels of structural self-organization.

The intramolecular self-organization necessary to induce a molecule to fold into a specific conformation is driven by the cooperative interplay of multiple molecular recognition processes such as hydrogen-bonding, van der Waals, electrostatic, and solvophobic interactions.[18] Noncovalent interactions have been exploited to promote intermolecular dendrimer self-assembly; however, the effect of intramolecular interactions such as hydrogen-bonding on dendrimer conformation has received little attention.[19] For example, Percec has prepared a series of monodendrons that assemble into liquid crystalline mesophases as a consequence of multiple, weak, intermolecular interactions.[20] Similarly, Zimmerman exploited intermolecular hydrogen-bonding interactions to drive dendrimer self-assembly.[21] Although noncovalent interactions, especially hydrogen-bonding interactions,[22] have been used to direct the intramolecular folding of linear oligomers, termed "foldamers," into helical conformations,[23] attractive forces such as hydrogen-bonding have not been exploited as a method to create secondary structural order in chiral dendrimers. Recently, we described a series of achiral dendrons whose conformational properties were restricted through the intervention of *intra*molecular hydrogen-bonding and electrostatic interactions present in the AB_2 building block.[24]

(14) (a) Chaumette, J.-L.; Laufersweiler, M. J.; Parquette, J. R. *J. Org. Chem.* **1998**, *63*, 9399. (b) Rohde, J. M.; Parquette, J. R. *Tetrahedron Lett.* **1998**, *39*, 9161.

(15) (a) Lellek, V.; Stibor, I. *J. Mater. Chem.* **2000**, *10*(5), 1061. (b) Rosini, C.; Superchi, S.; Peerlings, H. W. I.; Meijer, E. W. *Eur. J. Org. Chem.* **2000**, (1), 61. (c) Peerlings, H. W. I.; Meijer, E. W. *Eur. J. Org. Chem.* **1998**, *573*, 3. (d) Chen, Y.-M.; Chen, C.-F.; Xi, F. *Chirality* **1998**, *10*, 661. (e) Chen, Y.-M.; Chen, C.-F.; Xi, F. *Chirality* **1998**, *10*(7), 661.

(16) (a) Peerlings, H. W. I.; Trimbach, D. C.; Meijer, E. W. *Chem. Commun.* **1998**, 497. (b) Peerlings, H. W. I.; Struijk, M. P.; Meijer, E. W. *Chirality* **1998**, *10*, 46.

(17) For are recent review of studies relevant to the conformational behavior of dendrimers, see: Bosman, A. W.; Janssen, H. M.; Meijer, E. W. *Chem. Rev.* **1999**, *99*, 1665.

(18) (a) Buckingham A. D. In *Principles of Molecular Recognition*; Buckingham, A. D., Legon, A. C., Roberts, S. M., Eds.; Chapman and Hall: New York, 1993; p 1. (b) *Molecular Design and Bioorganic Catalysis*; Wilcox, C. S., Hamilton, A. D., Eds.; North Atlantic Treaty Organization. Scientific Affairs Division; Kluwer Academic Publishers: Dordrecht; Boston, 1996. (c) Vögtle, F.; Alfter, F. *Supramolecular Chemistry: An Introduction*; J. Wiley: Chichester; New York, 1991. (d) Delaage, M. *Molecular Recognition Mechanisms*; VCH Publishers:New York, NY, Lavoisier-Tec & Doc:Paris, France, 1991. (e) Lawrence, D. S.; Jiang, T.; Levett, M. *Chem. Rev.* **1995**, *95*, 2229. (f) Lindsey, J. S. *New J. Chem.* **1991**, *15*, 153.

(19) Noncovalent interactions at the periphery of dendrimers have been reported to reduce backfolding. For a discussion, see ref 17.

(20) (a) Percec, V.; Johansson, G.; Ungar, G.; Zhou, J. *J. Am. Chem. Soc.* **1996**, *118*, 9855. (b) Balagurusamy, V. S. K.; Ungar, G.; Percec, V.; Johansson, G. *J. Am. Chem. Soc.* **1997**, *119*, 1539. (c) Hudson, S. D.; Jung, H. T.; Percec, V.; Cho, W. D.; Johansson, G.; Ungar, G.; Balagurusamy, V. S. K. *Science* **1997**, *278*, 449. (d) Percec, V.; Cho, W. D.; Mosier, P. E.; Ungar, G.; Yeardley, D. J. P. *J. Am. Chem. Soc.* **1998**, *120*, 11061. (e) Percec, V.; Ahn, C. H.; Ungar, G.; Yeardley, D. J. P.; Moller, M.; Sheiko, S. S. *Nature* **1998**, *391*, 161. (f) Percec, V.; Ahn, C.-H.; Bera, T. K.; Ungar, G.; Yeardley, D. J. P. *Chem. Eur. J.* **1999**, *5*, 1070.

(21) (a) Zimmerman, S. C.; Zeng, F.; Reichert, D. E. C.; Kolotuchin, S. V. *Science* **1996**, *271*, 1095. (b) Thiyagarajan, P.; Zeng, F.; Ku, C. Y.; Zimmerman, S. C. *J. Mater. Chem.* **1997**, *7*, 1221. (c) Suarez, M.; Lehn, J.-M.; Zimmerman, S. C.; Skoulios, A.; Heinrich, B. *J. Am. Chem. Soc.* **1998**, *120*, 9526.

(22) For a review of hydrogen bonding in natural and synthetic peptides, see: Karle, I. L. *J. Mol. Struct.*, **1999**, *474*; 103.

(23) For an excellent review, see: (a) Gellman, S. H. *Acc. Chem. Res.* **1998**, *31*, 173. Hydrogen-bond driven foldamers, see: (b) Applequist, J.; Bode, K. A.; Appella, D. H.; Christianson, L. A.; Gellman, S. H. *J. Am. Chem. Soc.* **1998**, *120*, 4891. Solvophobically driven foldamers: (c) Gin, M. S.; Moore, J. S. *Org. Lett.* **2000**, *2*, 135. (d) Gin, M. S.; Yokozawa, T.; Prince, R. B.; Moore, J. S. *J. Am. Chem. Soc.* **1999**, *121*, 2643. (e) Prince, R. B.; Okada, T.; Moore, J. S. *Angew. Chem., Int. Ed.* **1999**, *38*, 233. (f) Nelson, J. C.; Saven, J. G.; Moore, J. S. Wolynes, P. G. *Science* **1997**, *277*, 1793.

(24) Huang, B.; Parquette, J. R. *Org. Lett.* **2000**, *2*, 239.

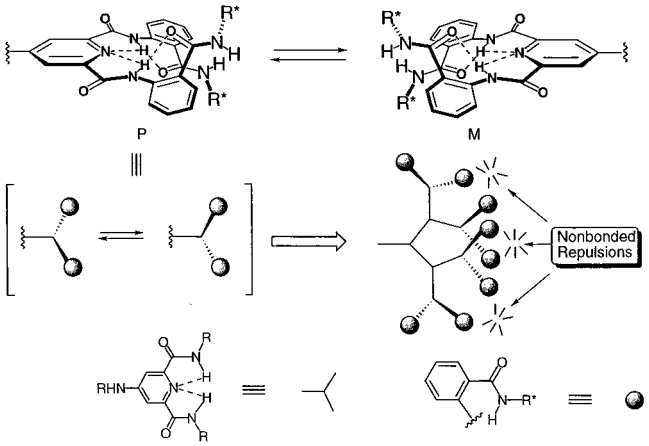

Figure 1. Perturbation of helical conformational equilibrium through nonbonded interactions in an intramolecularly hydrogen-bonded dendron.

In the present work, we demonstrate that hydrogen-bonding interactions direct the folding ability of chiral monodendrons; however, the development of a stable, helical secondary structure at the periphery of a monodendron requires concomitant hydrophobic packing interactions that increase with dendrimer generation and decreasing solvent quality.

Results and Discussion

Design Considerations. Monodendrons up to the third generation were constructed using 4-aminopyridine-2,6-dicarboxamide as the branching AB_2 unit to preorganize the interior of the dendrons through intramolecular hydrogen bonding interactions, and chiral, nonracemic anthranilamide groups were employed as termini. Pyridine-2,6-dicarboxamide derivatives exist in a conformation that places the amide NH groups in close proximity to the pyridine-*N* due to intramolecular hydrogen bonding and repulsive electrostatic interactions between the amide oxygens (Figure 1).[25] These hydrogen-bonding interactions, in conjunction with the preference of the terminal amides to exist in an *s*-trans conformation, constrain the system such that the terminal anthranilamide substituents are positioned above and below the plane of the molecule resulting in a local helical structure. Hamilton exploited this preference to enforce a turn in a series of oligoanthranilamides to create a helical "foldamer."[26] However, Borovik observed that, although chiral anthranilamides linked through a pyridine-2,6-dicarboxamide produced a helical conformation in the resultant molecule, the sense of helical chirality was not influenced by the chiral terminal substituent in the solid state or in solution.[27]

We hypothesized that, provided the monodendrons were conformationally constrained by intramolecular hydrogen-bonding interactions as shown in Figure 1, pairwise nonbonded interactions between adjacent termini at higher generations would facilitate the transmission of a single helical conformation across the surface of the dendrimer through a correlated propeller-like rotation of the peripheral anthranilamide groups.[28] Each pair of termini, considered as "blades," should twist in the same sense to minimize steric repulsions, thereby coupling the motions and conformations of each pair of termini. If such sympathetic motion were operative, the helical preference of each anthranilamide pair would be amplified by the presence of adjacent pairs through pairwise nonbonded interactions. Therefore, the equilibria interconverting the two diastereomeric helical conformations of each pair of terminal anthranilamides should increasingly favor a single helical conformation with increasing generation. This hypothesis is supported by reports demonstrating that intermolecular aggregation and template-directed intramolecular aggregation of α-helical peptide blocks enhances the stability of the α-helical conformation relative to that of the monomeric peptide block.[29] In these systems, secondary structure is stabilized through inter- or intramolecular hydrophobic packing interactions that correlate the conformations of each peptide block. These packing interactions should occur likewise in the monodendrons, provided that the terminal anthranilamide groups are held in close proximity by the hydrogen-bonding interactions. An X-ray structure of a second generation dendron displaying methyl anthranilate groups at the periphery supports this supposition; however, the presence of sterically unencumbered methyl ester termini generated insufficient nonbonded interactions to induce a helical disposition of the terminal groups.[24] Therefore, a relatively large aminodiol ((1*S*,2*S*)-(+)-thiomicamine) was used as the chiral terminal substituent for this series of dendrons.

Dendron Synthesis and Characterization. Accordingly, 4-chloropyridine-2,6-dicarbonyl chloride, **1**, was chosen as the branching monomer wherein convergent generational growth was accomplished using amide bond-forming reactions with the acid chlorides and focal point activation occurred by NaN_3 displacement of the 4-chloro group followed by hydrogenation. The AB_2 unit, **1**, was prepared by treating chelidamic acid with PCl_5 at 100 °C and was purified by sublimation. Synthesis of the dendrons proceeded in a convergent fashion wherein thiomicamine **2** was selectively *N*-acylated with 2-nitrobenzoyl chloride then peracetylated with acetic anhydride (Scheme 1). Hydrogenation over Pd−C followed by reaction with **1** afforded the first generation dendron, **5a**, displaying a chloro group at the focal point. Focal activation was achieved through displacement of the chloro group with NaN_3 in DMF at 50 °C followed by hydrogenation over Pd−C. Growth to the second generation occurred by amidation of **1** in pyridine and repetition of the NaN_3 displacement−hydrogenation activation sequence followed by condensation with **1** afforded the third generation dendron **7**. Characterization with regard to molecular weight, structure, and dispersity was accomplished by EI, FAB or MALDI-TOF MS, and NMR. The proton NMR spectra of the second and third generation dendrons (**6**, **7**) were broad and structureless in $CDCl_3$ but well-resolved in DMSO-d_6. We observed this behavior previously in a third generation dendron containing dodecyl ester termini and attribute it to aggregation that occurs in nonpolar solvents but not in polar solvents.[24]

Optical Rotation Studies. Optical rotation studies were carried out to provide preliminary information concerning the presence or absence of chiral substructures. However, changes in aggregation state can give rise to large variations in optical rotatory power.[30] Therefore, optical rotations were recorded in

(25) For X-ray crystal structures, see: (a) Newkome, G. R.; Fronczek, F. R.; Kohli, D. K. *Acta Crystallogr.* **1981**, *B37*, 2114. (b) Alcock, N. W.; Moore, P.; Reader, J. C.; Roe, S. M. *J. Chem. Soc., Dalton Trans.* **1988**, 2959.

(26) (a) Hamuro, Y.; Geib, S. J.; Hamilton, A. D. *J. Am. Chem. Soc.* **1997**, *119*, 10587. (b) Hamuro. Y.; Geib, S. J.; Hamilton, A. D. *J. Am. Chem. Soc.* **1996**, *118*, 7529.

(27) Yu, Q.; Baroni, T. E.; Liable-Sands, L.; Rheingold, A. L.; Borovik, A. S. *Tetrahedron Lett.* **1998**, *39*, 6831.

(28) For a discussion of the correlated rotation in molecular propellers, see: Mislow, K. *Acc. Chem. Res.* **1976**, *26*, 6.

(29) (a) Mutter, M.; Vuilleumier, S. *Angew. Chem., Int. Ed. Engl.* **1989**, *5*, 535. (b) Sasaki, T.; Kaiser, E. T. *J. Am. Chem. Soc.* **1989**, *111*, 380. (c) Ghadiri, M. R.; Soares, C.; Choi, C. *J. Am. Chem. Soc.* **1992**, *114*, 825. (d) Dawson, P. E.; Kent, S. B. H. *J. Am. Chem. Soc.* **1993**, *115*, 7263. (e) Higashi, N.; Koga, T.; Niwa, N.; Niwa, M. *Chem. Commun.* **2000**, 361.

(30) Eliel, E. L.; Wilen, S. H. *Stereochemistry of Organic Compounds*; Wiley: New York, 1994; p 1076.

Scheme 1[a]

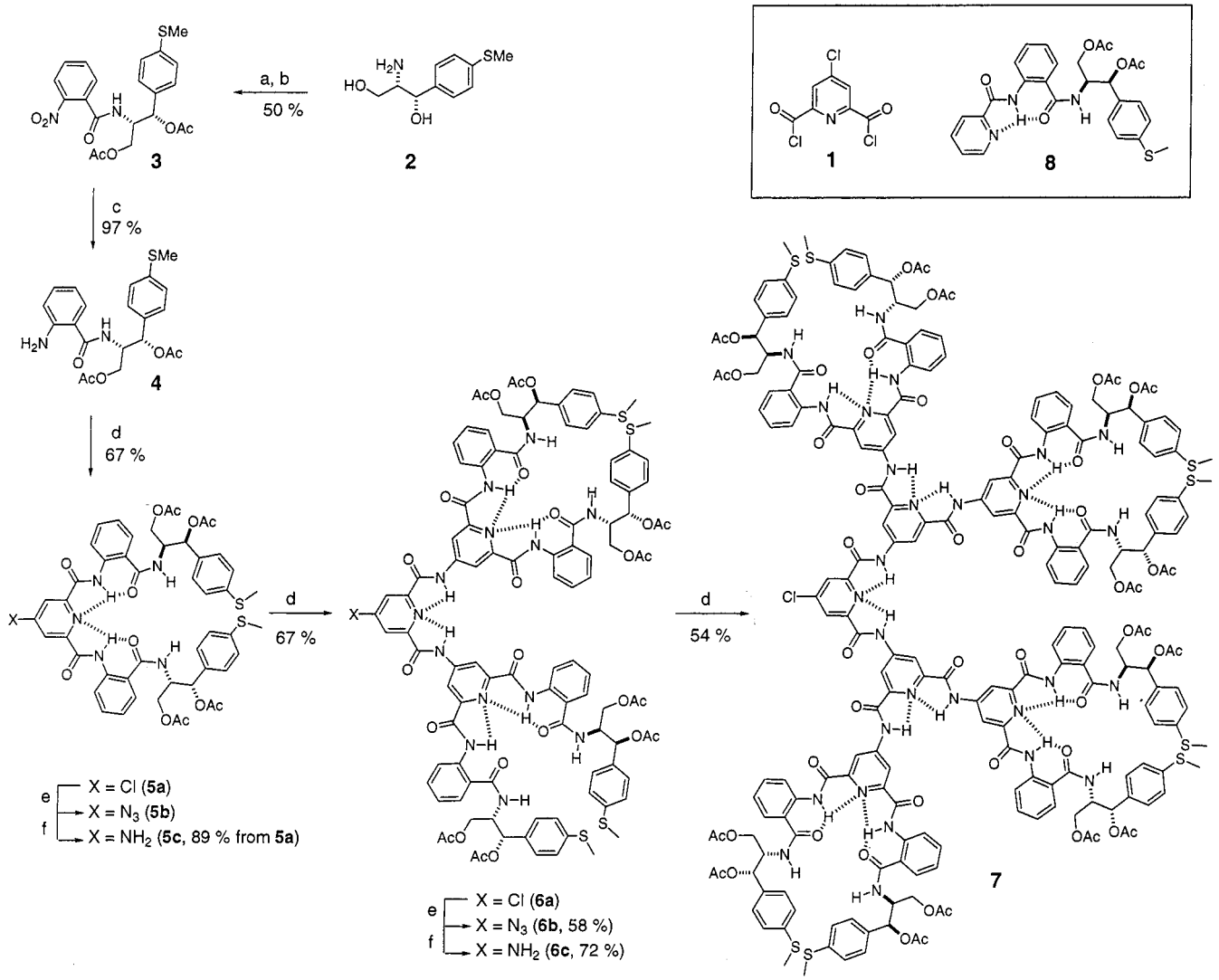

Key: (a) 2-$NO_2C_6H_4COCl$, pyr., DMAP. (b) Ac_2O, pyr., DMAP. (c) H_2, Pd−C. (d) **1**, CH_2Cl_2−pyr. (e) NaN_3, DMF, 50 °C. (f) H_2, Pd−C.

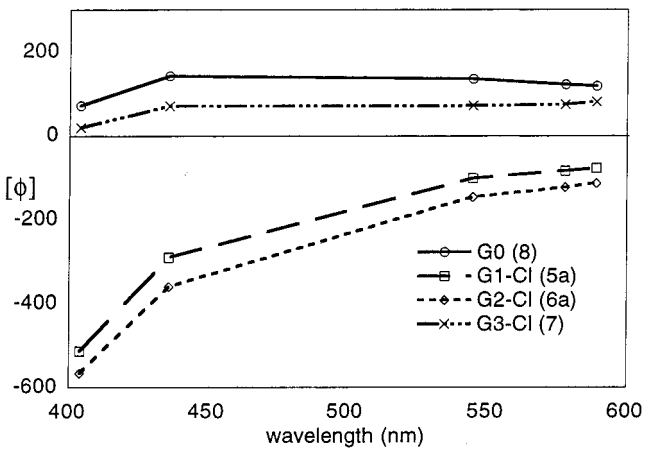

Figure 2. Molar ORD spectra (normalized for the number of chiral termini) for **5a** ($1.00\cdot10^{-2}$ M), **6a** ($4.73\cdot10^{-3}$ M), **7** ($2.29\cdot10^{-3}$ M), and **8** ($1.92\cdot10^{-2}$ M) in DMSO at 23 °C.

DMSO at 23 °C because ^{1}H NMR analysis indicated that the dendrons were monomeric in this solvent. Optical rotatory dispersion (ORD) spectra, normalized for concentration and the number of chiral termini, are presented in Figure 2. The sign and absolute magnitude of the rotations were not linearly dependent on dendrimer generation. For example, changes in the sign of rotation were observed going from the zeroth (**8**) to first (**5a**) and from the second (**6a**) to third generations (**7**). The nonlinearity of rotation magnitude and sign suggested that chiral secondary structure was developing in the dendrons; therefore, further chiroptical studies were performed to gain specific information concerning the conformational equilibria present in the dendrons.

Circular Dichroism Studies. Circular dichroism (CD) was investigated to determine the influence of chiral terminal groups on the conformational equilibrium that interconverts the two diastereomeric helical conformations relating each pair of anthranilamide termini on the dendrons (Figure 1). To provide a control compound incapable of developing helical secondary structure, **4** was acylated with pyridine-2-carboxylic acid affording G0-control **8**. All spectra were carried out at the same concentration for a given generation and were normalized with respect to concentration and the number of chiral terminal groups so that differences in the CD spectra would reveal perturbations of conformational equilibria. The CD spectrum of the G0 control, **8**, and the first generation dendron **5a** in CH_2Cl_2 at 25 °C revealed two Cotton Effects (CE) in the range of 240−400 nm (Figure 3). Both compounds displayed a positive CE at 260

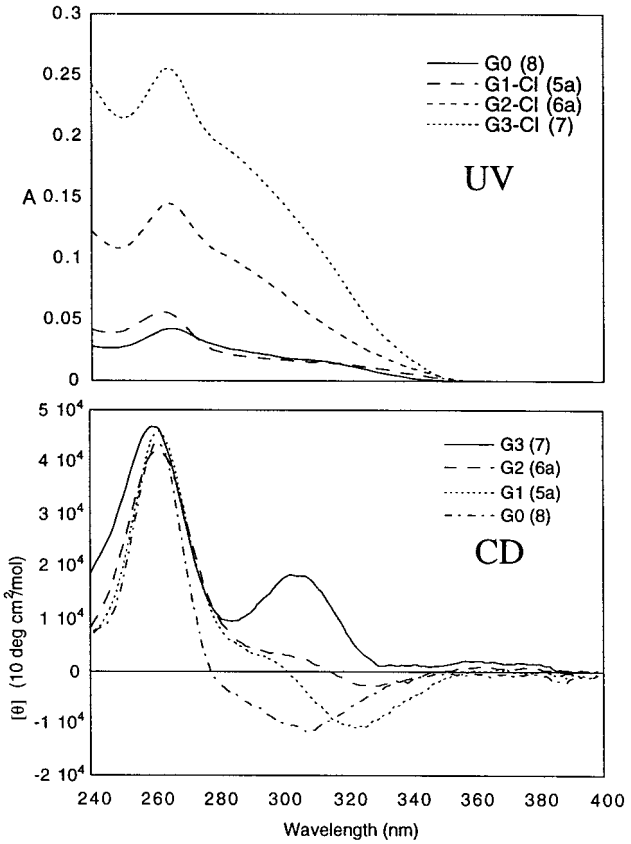

Figure 3. UV (normalized to 1.6 μM) and CD spectra of **5**−**8** in CH_2Cl_2 at 25 °C. Concentrations for CD: **8**, $1.9\cdot10^{-5}$ M; **5a**, $8.0\cdot10^{-6}$ M; **6a**, $3.7\cdot10^{-6}$ M; **7**, $1.6\cdot10^{-6}$ M.

nm (Band A) and a negative CE at 310 nm for **8** and 316 nm for **5a** (Band B). Although the shorter wavelength UV transitions at 260 nm are due to overlapping transitions of several chromophores, the longer wavelength transition (Band B) can be attributed to a $\pi\rightarrow\pi^*$ transition of the 2-acylaminobenzamide chromophore at the periphery of the dendron (see TDDFT-B3LYP calculations, vide infra). All of the CEs were of comparable intensity and lacked any apparent intrachromophore excitonic coupling. However, the shape of Band B CEs were slightly different. As will become apparent at higher generations, the shape of the CE for this transition in **5a** is due to a weak excitonic coupling between the two anthranilamide chromophores not present in **8**. The spectra of **8** and **5a** were insensitive to solvent and temperature (Figure 4).[31] Therefore, we conclude that the chiral, nonracemic terminal groups in **5a** have little or no influence on the position of the conformational equilibrium interconverting the two helical antipodes.

Comparison of the CD spectra of first and second generation dendrons, **5a** and **6a**, revealed significant differences in the transitions associated with Band B in CH_2Cl_2 at 25 °C. Although G1 dendron **5a** exhibited a negative CE centered at 316 nm corresponding to the λ_{max} of this transition, the second generation dendron **6a** showed an excitonically coupled transition with a positive CE at 300 nm, a negative CE at 327 nm, and a zero-crossing at 316 nm, corresponding to negative chirality as defined by Nakanishi and Harada (Figure 3).[32] Time-dependent density-functional (TDDFT) methods[33] were applied to 2-acetamido-*N*-methylbenzamide to model the terminal 2-acylaminobenzamides responsible for the transition at 316 nm using the three-parameter Lee−Yang−Parr (B3LYP) functional.[34] The structure was constrained in the calculation to a planar, intramolecularly hydrogen-bonded conformer similar to the conformation of this subunit in the dendrons.[35] The lowest-energy transition corresponded to a $\pi\rightarrow\pi^*$ transition at 302 nm in reasonable agreement with the experimental value of this electronic absorption (Table 1).[36] The electric transition moment associated with this transition runs along the axis containing C3 and C6 of the anthranilamide ring. Therefore, the absolute sense of helical chirality between each pair of anthranilamide chromophores can be assigned to be M as shown in Figure 5 using the exciton chirality method pneumonic.

The conformational origin of the exciton couplet is supported by the extreme solvent and temperature sensitivity of this couplet. For example, the intensity of the exciton couplet increases significantly in acetonitrile and dramatically in hexane/CH_2Cl_2 (2:1) (Figure 6).[37] Although CH_2Cl_2 is a good solvent for **5**−**8**, all of the dendrons are sparingly soluble in acetonitrile and insoluble in hexane, which requires CH_2Cl_2 as a cosolvent to dissolve the dendrons. Since the intensity of the couplet increases with decreasing solvent quality, a solvophobic compression of **6a** must be occurring that increases nonbonded packing interactions at the periphery and reduces conformational freedom. This interpretation is consistent with several theoretical[38] and experimental[39] studies, indicating that dendrimers collapse in poor solvents and expand in good solvents. Solvophobic compression perturbs the conformational equilibrium of the terminal anthranilamides so that a single helical conformation becomes increasingly favored with decreasing solvent quality.[40] Further, the addition of 1% ethanol to the CH_2Cl_2 solution of

(31) In acetonitrile, G0 (**8**) exhibited a slightly higher intensity CE at 310 nm. The origin of this effect is not known.

(32) Harada, N.; Nakanishi, K. O. *Circular Dichroic Spectroscopy: Exciton Coupling in Organic Stereochemistry*; University Science Books: Mill Valley, CA, 1983.

(33) The TDDFT-B3LYP calculations were run as implemented in: Frisch, M. J.; Trucks, G. W.; Schlegel, H. B.; Scuseria, G. E.; Robb, M. A.; Cheeseman, J. R.; Zakrzewski, V. G.; Montgomery, J. A., Jr.; Stratmann, R. E.; Burant, J. C.; Dapprich, S.; Millam, J. M.; Daniels, A. D.; Kudin, K. N.; Strain, M. C.; Farkas, O.; Tomasi, J.; Barone, V.; Cossi, M.; Cammi, R.; Mennucci, B.; Pomelli, C.; Adamo, C.; Clifford, S.; Ochterski, J.; Petersson, G. A.; Ayala, P. Y.; Cui, Q.; Morokuma, K.; Malick, D. K.; Rabuck, A. D.; Raghavachari, K.; Foresman, J. B.; Cioslowski, J.; Ortiz, J. V.; Stefanov, B. B.; Liu, G.; Liashenko, A.; Piskorz, P.; Komaromi, I.; Gomperts, R.; Martin, R. L.; Fox, D. J.; Keith, T.; Al-Laham, M. A.; Peng, C. Y.; Nanayakkara, A.; Gonzalez, C.; Challacombe, M.; Gill, P. M. W.; Johnson, B. G.; Chen, W.; Wong, M. W.; Andres, J. L.; Head-Gordon, M.; Replogle, E. S.; Pople, J. A. *Gaussian 98*, revision A.7; Gaussian, Inc.: Pittsburgh, PA, 1998.

(34) (a) Bauernschmitt, R.; Ahlrichs, R. *Chem. Phys. Lett.* **1996**, *256*, 454. (b) Stratmann, R. E.; Scuseria, G. E.; Frisch, M. J. *J. Chem. Phys.* **1998**, *109*, 8218. (c) Foresman, J. B.; Head-Gordon, M.; Pople, J. A.; Frisch, M. J. *J. Phys. Chem.* **1992**, *96*, 135. Recently, the circular dichroism of helicenes has been investigated using TDDFT methods, see: (d) Furche, F.; Ahlrichs, R.; Wachsmann, C.; Weber, E.; Sobanski, A.; Vögtle, F.; Grimme, S. *J. Am. Chem. Soc.* **2000**, *122*, 1717.

(35) The conformation shown in Figure 1 provides a specific orientation of the 2-acylaminobenzamide chromophore with respect the C_2 axis of the molecule. It is based upon X-ray crystal structures of closely related structures (see refs 24−27).

(36) The transitions in Table 1 were assigned as $\sigma\rightarrow\pi^*$ or $\pi\rightarrow\pi^*$ on the basis of the symmetry of the ground and excited-state molecular orbitals that contribute to the transition. (See Supporting Information).

(37) That the shorter branch of the couplet is stronger than the longer-wavelength branch is likely due to mixing of the couplet transition with other transitions. The degree of mixing could be expected to increase as the chromophores become more congested at higher generations. For a discussion, see: Gottarelli, G.; Mason, S. F.; Torre, G. *J. Chem. Soc. B* **1970**, 1349.

(38) (a) Murat, M.; Grest, G. S. *Macromolecules* **1996**, *29*, 9(4), 1278. (b) Scherrenberg, R.; Coussens, B.; van Vliet, P.; Edouard, G.; Brackman, J.; de Brabander, E.; Mortensen, K. *Macromolecules* **1998**, *31*, 1(2), 456. (c) Welch, P.; Muthukumar, M. *Macromolecules* **1998**, *31*, 1(17), 5892.

(39) De Backer, S.; Prinzie, Y.; Verheijen, W.; Smet, M.; Desmedt, K.; Dehaen, W.; De Schryver, F. C. *J. Phys. Chem. A* **1998**, *102*(28), 5451.

(40) For an example of a solvophobically driven folding event in phenylacetylene oligomers see refs 23 c−f.

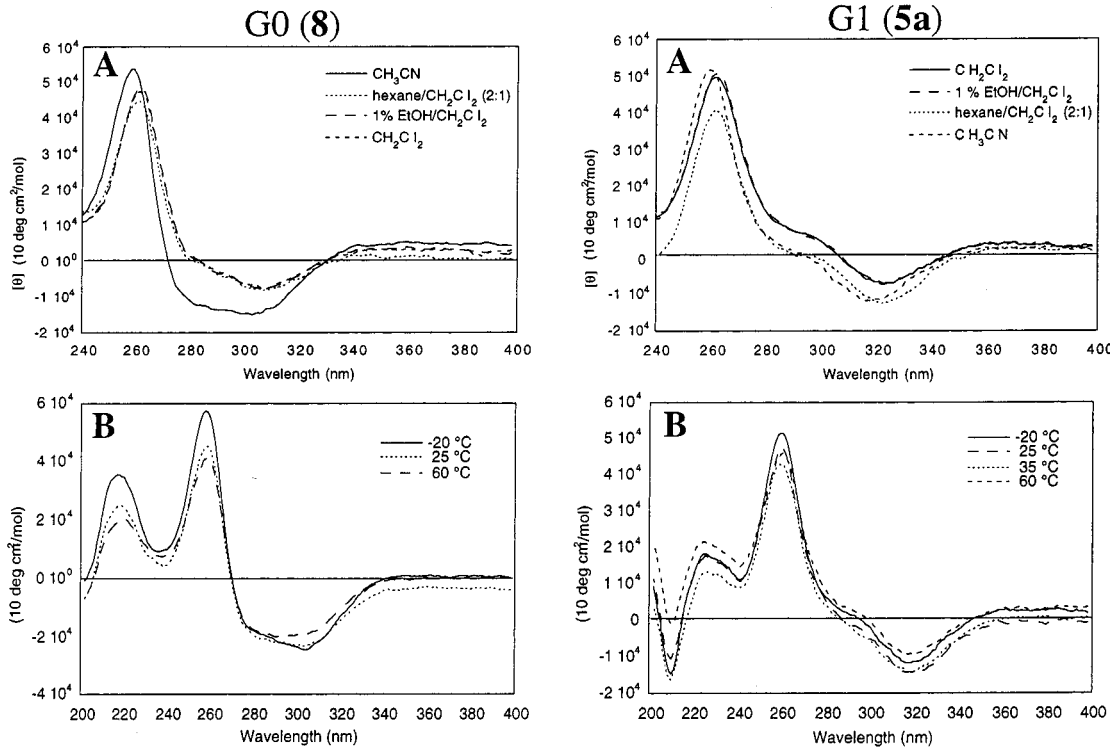

Figure 4. CD of G0, **8**, and G1 dendron, **5a**, as function of (a) solvent at 25 °C, (b) temp in CH_3CN. [**5a**] = $8.0 \cdot 10^{-6}$ M, [**8**] = $1.9 \cdot 10^{-5}$ M.

Table 1. Electric Transition Moments of 2-Acetamido-*N*-methylbenzamide

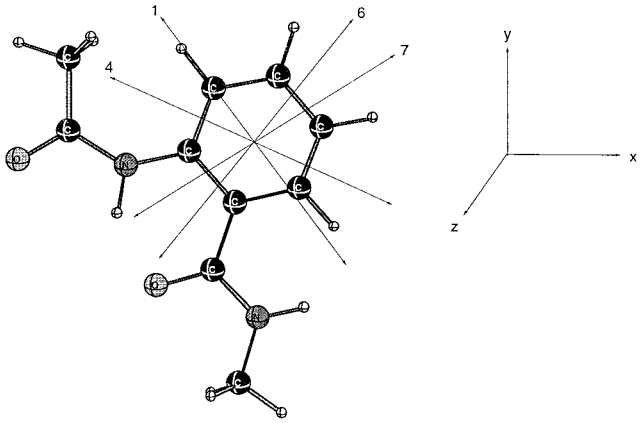

	type[b]	wavelength (nm)	oscillator strength	transition electric dipole moments		
				x	*y*	*z*
1	$\pi \rightarrow \pi^*$	302.2	0.1280	0.6880	−0.8944	0.0000
2	$\sigma \rightarrow \pi^*$	272.3	0.0003	0.0000	0.0000	0.0533
3	$\sigma \rightarrow \pi^*$	263.2	0.0000	0.0000	0.0075	0.0000
4	$\pi \rightarrow \pi^*$	246.1	0.2171	1.2192	−0.5217	0.0000
5	$\sigma \rightarrow \pi^*$	238.1	0.0002	0.0000	0.0000	0.0378
6	$\pi \rightarrow \pi^*$	232.8	0.1047	−0.5623	−0.6975	0.0000
7	$\pi \rightarrow \pi^*$	211.6	0.3312	−1.2985	−0.7882	0.0000
8	$\sigma \rightarrow \pi^*$	211.2	0.0000	0.0000	0.0000	−0.0106
9	$\pi \rightarrow \pi^*$	208.0	0.0413	0.0316	−0.5309	0.0000
10	$\pi \rightarrow \pi^*$	201.0	0.1217	0.8546	0.2742	0.0000

[a] Calculated using TDDFT-B3LYP implemented in Gaussian 98. [b] Assigned by inspection of the symmetry of the molecular orbitals associated with the transition (see Supporting Information).

6a destroys the excitonic interaction resulting in a simple CE centered at 316 similar to that observed at the first generation; however, it has little effect on the CD spectrum in CH_3CN or hexane/CH_2Cl_2 (2:1). Presumably, this is due to disruption of the intramolecular hydrogen-bonding interactions that partially stabilize the helical conformation. Heating the sample in acetonitrile to 60 °C completely destroys the exciton couplet and is consistent with a thermal unfolding process occurring; however, cooling to −20 °C dramatically increases amplitude of the couplet at 316 nm and the CE at 260 nm. Interestingly, the shape and amplitude of the transition between 200 and 240 nm at −20 °C changes relative to the CD observed at 35 and 60 °C, suggesting that the chiral terminal groups are perturbing the conformation of the internal regions of the dendron at this temperature. However, due to the presence of overlapping transitions in this region of the absorption spectrum, this effect cannot be fully rationalized. In hexane/CH_2Cl_2 (2:1), the temperature sensitivity is much less pronounced in accord with the increased helical conformational bias in this solvent system. On the basis of these observations, we can conclude that the increased nonbonded repulsions present at the second generation contribute significantly to the stabilization of the secondary structure that develops across the periphery of the dendron. However, the expression of maximal conformational order requires a concurrent solvophobic compression in conjuction with low temperatures to enhance intramolecular packing interactions.

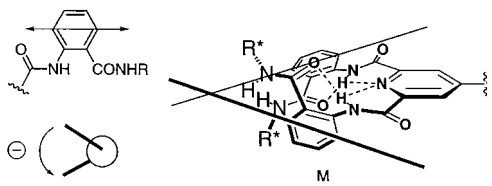

Figure 5. Assignment of absolute helicity of terminal anthranilamides.

At the third generation (**7**), the intensity of the couplet was invariant with solvent and displayed an intensity similar to that observed for **6a** in hexane, indicating that the helical bias was driven predominantly by the nonbonded repulsions and packing interactions associated with the increased number of terminal groups present at the third generation dendron (Figure 7).

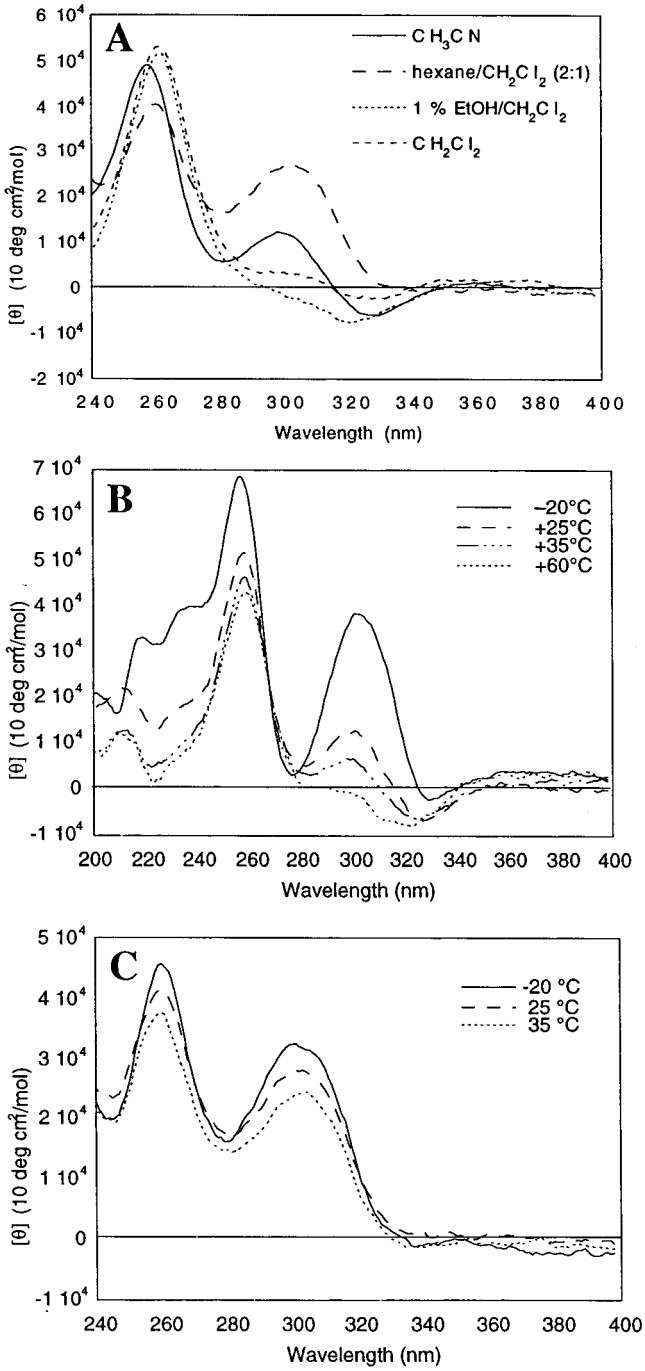

Figure 6. CD of G2 dendron, **6a**, as function of (a) solvent at 25 °C, (b) temp in CH_3CN, (c) temp in hexane/CH_2Cl_2 (2:1); [**6a**] = $3.7 \cdot 10^{-6}$ M.

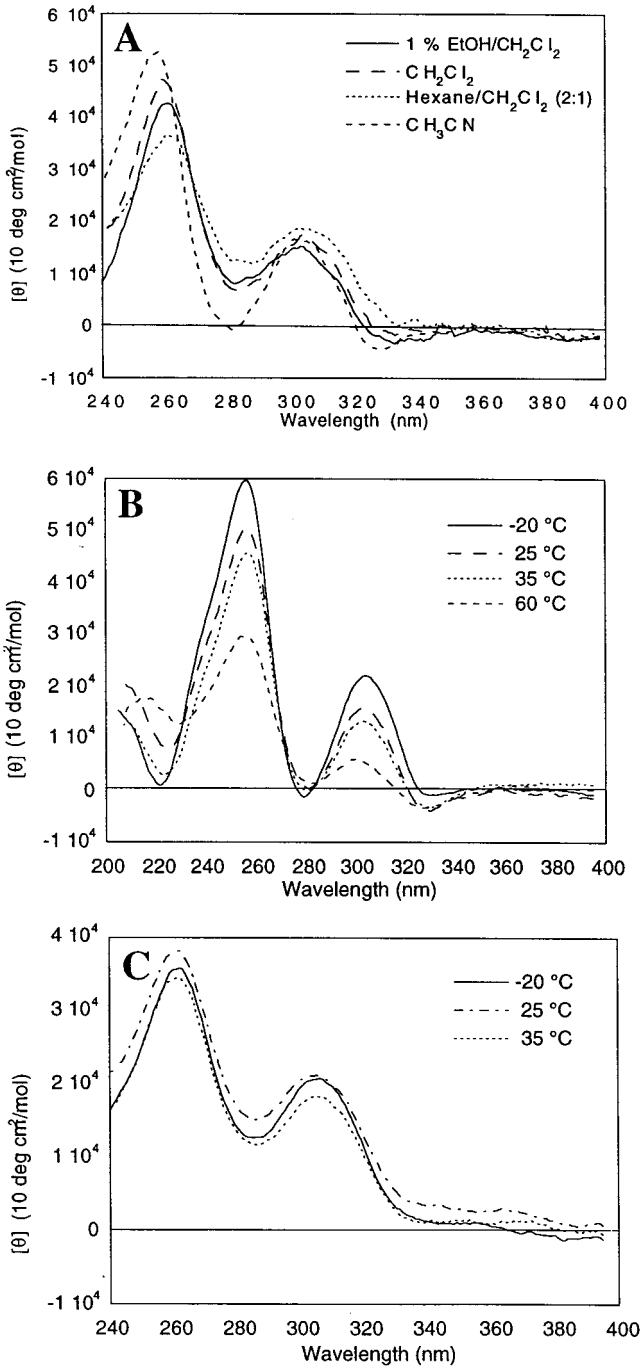

Figure 7. CD of G3 dendron, **7**, as function of (a) solvent at 25 °C, (b) temp in CH_3CN, (c) temp in hexane/CH_2Cl_2 (2:1); [**7**] = $1.6 \cdot 10^{-6}$ M.

However, the temperature sensitivity of the couplet was higher in CH_3CN than in hexane/CH_2Cl_2 (2:1) as observed for **6a**. Whereas **6a** was entirely unfolded in CH_3CN at 60 °C, **7** maintained the excitonic couplet, albeit with decreased intensity under these conditions. Further, the addition of 1% ethanol to CH_2Cl_2 solution of **7** slightly reduced the intensity of the couplet but did not change the shape of the couplet. These observations indicate that conformational order is intrinsically more stable at the third generation than at either the first or second generations.

Effect of Aggregation. The tendency of the second and third generation dendrons to aggregate suggest that aggregation may play a role in the conformational equilibria and CD spectra of these dendrons.[41] Therefore, the spectra were recorded for **6a** and **7** as a function of concentration in CH_2Cl_2, CH_3CN and hexane/CH_2Cl_2 (2:1) (Figure 8).[42] In the region between 230 and 400, only small changes were observed for **6a** and **7** over a 10-fold concentration range; however a few points are noteworthy. In CH_2Cl_2 and CH_3CN, the excitonic couplet

(41) For examples in which CD is enhanced by aggregation, see: (a) Palmans, A. R. A.; Vekemans, J. A. J. M.; Havinga, E. E.; Meijer, E. W. *Angew. Chem., Int. Ed. Engl.* **1997**, *36*, 2648. (b) Nuckolls, C.; Katz, T. J.; Verbiest, T.; Van Elshocht, S.; Kuball, H. G.; Kiesewalter, S.; Lovinger, A. J.; Persoons, A. *J. Am. Chem. Soc.* **1998**, *120*, 8656. (c) Nuckolls, C.; Katz, T. J.; Castellanos, L. *J. Am. Chem. Soc.* **1996**, *118*, 3767. (d) Huang, D. W.; Matile, S.; Berova, N.; Nakanishi, K. *Heterocycles* **1996**, *42*, 723. (e) Jodál, I.; Kovács, Ott, J.; Snatzke, G. *Chem. Ber.* **1989**, *122*, 1207.

(42) The poor solubility of **7** in hexane/CH_2Cl_2 (21) did not permit a sufficient concentration range to be accessible; therefore, concentration-dependent CD spectra could not be recorded in this solvent.

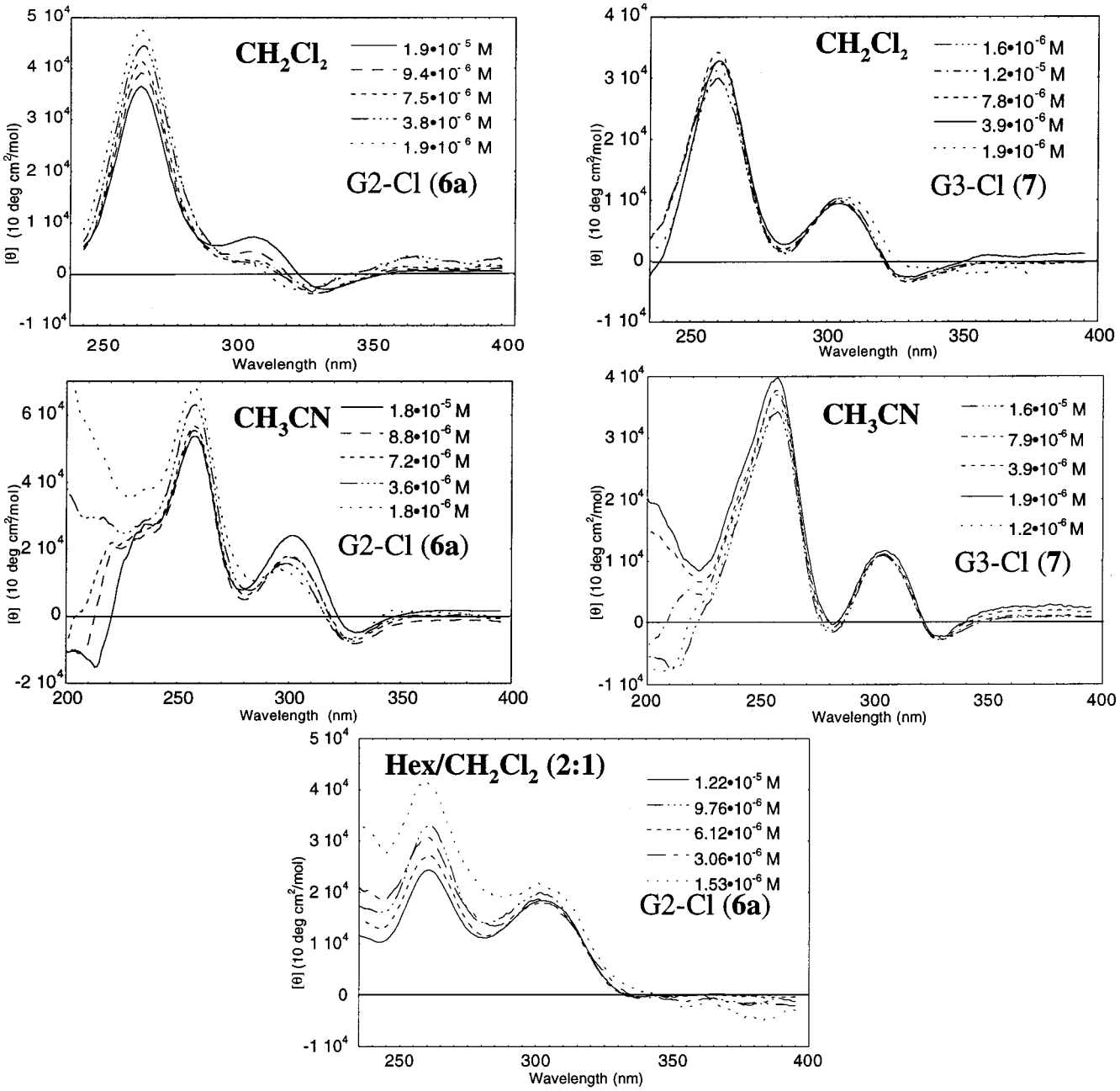

Figure 8. CD of G2-C1 (**6a**) G3-C1 (**7**) as function of concentration at 25 °C.

centered at 316 nm increased slightly with increasing concentration; however, in hexane/CH_2Cl_2 (2:1) for G2-Cl, and for G3-Cl in all solvents, the intensity of the couplet remained relatively constant. The small increase in intensity of couplet for G2-Cl may be associated with intermolecular packing interactions that increase with greater aggregation. Intermolecular aggregation/packing has been observed to enhance the stability of secondary structure in proteins[29] and may be operative to a small extent in the dendrons under conditions in which the secondary structure is less stable as for G2-Cl in CH_2Cl_2 and CH_3CN. In contrast, the CE at 260 nm increases with decreasing concentration for G2-Cl and the region below 230 nm (only observable in CH_3CN) varies significantly with concentration. Since several transitions contribute to the CD spectra at 260 nm and below 235 nm, it is not possible to determine the origin of this concentration dependence. However, we can conclude that the effect of aggregation on the excitonic interaction at 316 nm is small and that this couplet arises from intramolecular excitonic coupling and not from intermolecular excitonic interactions due to aggregation.

Conclusions

Intramolecular hydrogen bonding and electrostatic interactions in the pyridine-2,6-dicarboxamide subunit dominate the folding ability of these monodendrons; however, self-organization does not occur in the absence of nonbonded packing interactions that develop at the second and third generations. We hypothesize that these nonbonded interactions couple the motions and conformational preferences of each pair of terminal groups through their correlated rotations. The increased intramolecular packing of the terminal groups that occurs at higher generations of these intramolecularly hydrogen-bonded dendrons likely contributes significantly to the stabilization of the helical conformation at the periphery. Consequently, the helical conformational preference increases with increasing dendrimer generation and in poor solvents that enhance these nonbonded

interactions. Equilibration of diastereomeric helical conformations is rapid at the first generation in all solvents and at all temperatures investigated; however, at the second generation the equilibrium begins to bias a single diastereomeric helical conformation along the periphery that becomes maximal at low temperature and in poor solvents. At the third generation, the helical bias is intrinsically higher so that the conformational preference of the termini becomes much less sensitive to solvent and temperature, and the unfolding process becomes more difficult. Since the maximal intensity of the couplet and other CEs at low temperatures is similar in the second and third generation monodendrons, the source of conformational order can be attributed primarily to a shift in the conformational equilibria interconverting two helical orientations of a pair of anthranilamides.

Experimental Section

General. Melting points were determined in open capillaries and are uncorrected. ^{1}H NMR spectra were recorded at 250, 400, or 500 MHz and ^{13}C NMR spectra at 100 or 125 MHz. EI or FAB mass spectra were recorded at The Ohio State University Chemical Instrument Center. MALDI-TOF spectrometry was performed using 2,5-dihydroxybenzoic acid as the matrix in tetrahydrofuran (THF). Circular dichroism (CD) measurements were carried out on an Aviv 202 CD spectrometer, using optical grade solvents and quartz glass cuvettes with a 10 mm path length. Optical rotations were performed on a Perkin-Elmer 241 MC polarimeter at a concentration of 10 mg/mL ($c = 1$). All reactions were performed under an argon or nitrogen atmosphere. Dimethylformamide (DMF) was dried by distillation from barium oxide or magnesium sulfate, THF was distilled from sodium/benzophenone ketyl, and dichloromethane was distilled from calcium hydride. Chromatographic separations were performed on silica gel 60 (230−400 mesh, 60 Å) using the indicated solvents.

(1*S*,2*S*)-2-(2-Nitrobenzamido)-1-(4-methylthiophenyl)-1,3-propanediylbisacetate (3). To a stirred solution of (1*S*,2*S*)-(+)-thiomicamine, **2**, (10.24 g, 48.0 mmol) and 4-(dimethylamino)pyridine (DMAP) (1.17 g, 9.6 mmol) in 400 mL of pyridine, 2-nitrobenzoyl chloride (9.05 g, 48.8 mmol) was added dropwise via syringe over 3 h at 0 °C. After the addition was complete, acetic anhydride (19.6 g, 192 mmol) was added, and the solution was then stirred at 60 °C for 3 h. Pyridine was removed by distillation under reduced pressure and the resultant residue was dispersed in CH_2Cl_2 (400 mL). The CH_2Cl_2 solution was washed with 10% aqueous sulfuric acid (200 mL) and saturated aqueous sodium bicarbonate (100 mL) and then dried over $MgSO_4$ and concentrated in vacuo. Purification by flash chromatography (SiO_2) using a gradient going from 20:1 to 8:1 dichloromethane/ethyl acetate afforded [G0]-NO_2 **(3)** (10.61 g, 0.024 mmol, 50%) as a light yellow solid: mp 116−117 °C (CH_2Cl_2/EtOAc). ^{1}H NMR (400 MHz, $CDCl_3$) δ 2.02 (s, 3H), 2.07 (s, 3H), 2.42 (s, 3H), 3.88 (dd, $J = 5.2$, 11.7 Hz, 1H), 4.17 (dd, $J = 4.1$, 11.7 Hz, 1H), 4.76 (m, 1H), 5.90 (d, $J = 7.9$ Hz, 1H), 6.17 (d, $J = 9$ Hz, 1H), 7.19 (d, $J = 8.0$ Hz, 2H), 7.25 (d, $J = 8.0$ Hz, 2H), 7.29 (d, $J = 6$ Hz, 1H), 7.51 (t, 1H), 7.60 (t, 1H), 7.98 (d, $J = 8.1$ Hz, 1H); ^{13}C NMR (100 MHz, $CDCl_3$) 15.9, 21.1, 21.5, 53.4, 63.4, 74.3, 125.0, 127.0, 127.9, 128.9, 131.1, 132.9, 133.3, 134.2, 140.3, 146.9, 166.7, 171.1, 171.2 ppm; HRMS for $C_{21}H_{22}N_2O_7S$ (EI) (M^+): Calcd 446.1148; obsd 446.1144. Anal. Calcd for $C_{21}H_{22}N_2O_7S$: C, 56.49; H, 4.97; N, 6.27. Found: C, 56.25; H, 4.99; N, 6.16.

(1*S*,2*S*)-2-(2-Aminobenzamido)-1-(4-methylthiophenyl)-1,3-propanediylbisacetate (4). [G0]-NO_2 **(3)** (15.92 g, 36 mmol) was dissolved in 100 mL of ethyl acetate−methanol (1:1), and the solution was degassed by sparging with argon for 10 min. 10% Pd−C (1.59 g) was then added, and the mixture was hydrogenated at 1 atm H_2 pressure for 48 h at room temperature. The catalyst was then removed by filtration through a pad of Celite with ethyl acetate (400 mL). The ethyl acetate was removed in vacuo, and the resultant solid was passed through a short plug of silica gel using ethyl acetate affording [G0]-NH_2 **(4)** as a white waxy solid (14.34 g, 34 mmol, 97%): mp 146−148 °C (EtOAc). ^{1}H NMR (400 MHz, $CDCl_3$) δ 2.11 (s, 3H), 2.12 (s, 3H), 2.50 (s, 3H), 4.03 (dd, $J = 5.0$, 11.5 Hz, 1H), 4.19 (dd, $J = 4.5$, 11.5 Hz, 1H), 4.84 (m, 1H), 5.60 (bs, 2H), 6.06 (d, $J = 7.5$ Hz, 1H), 6.42 (d, $J = 9.0$ Hz, 1H), 6.73 (t, $J = 7.0$ Hz, 1H), 6.74 (d, $J = 7.5$ Hz, 1H), 7.28 (d, $J = 8.5$ Hz, 2H), 7.30−7.32 (m, 2H), 7.35 (d, $J = 8.3$ Hz, 2H); ^{13}C NMR (100 MHz, $CDCl_3$) 15.9, 21.2, 21.5, 52.6, 63.7, 74.4, 115.8, 117.1, 117.8, 127.0, 127.5, 127.9, 133.1, 133.6, 140.0, 149.3, 169.4, 171.0, 171.1 ppm; HRMS for $C_{21}H_{24}N_2O_5S$ (EI) (M^+): Calcd 416.1406; obsd 416.1406. Anal. Calcd for $C_{21}H_{24}N_2O_5S$: C, 60.56; H, 5.81; N, 6.73. Found: C, 60.53; H, 5.81; N, 6.68.

4-Chloro-pyridine-2,6-dicarbonyl Chloride (1).[24] Chelidamic acid monohydrate (1.81 g, 9 mmol) was treated with phosphorus pentachloride (5.62 g, 27 mmol) in toluene (20 mL) and then heated at reflux for 24 h. The toluene was removed by distillation at reduced pressure, and **1** was obtained by sublimation at 110 °C at 0.1 mmHg as a white solid (1.37 g, 63%). ^{1}H NMR (250 MHz, $CDCl_3$) δ 8.31 (s, 2H).

4-Chloro-2,6-bis[(2-(1*S*,2*S*)-1-(4-methylthiophenyl)-1,3-propanediyl-bisacetate) Carbamoylphenyl)carbamoyl]pyridine (5a). [G0]-NH_2 **(4)** (10.47 g, 25.14 mmol) and DMAP (0.154 g, 1.26 mmol) was dissolved in a mixture of CH_2Cl_2 (80 mL) and pyridine (20 mL). 4-chloro-pyridine-2,6-dicarbonyl chloride **(1)** (3.00 g, 12.58 mmol) in 13 mL CH_2Cl_2 was then added dropwise via syringe to this mixture over 60 min. After stirring at room temperature for 16 h, the mixture was taken up in CH_2Cl_2 (300 mL). The CH_2Cl_2 solution was washed with 10% aqueous sulfuric acid (300 mL) and saturated sodium bicarbonate solution (100 mL) and then dried over $MgSO_4$ and concentrated in vacuo. Purification by flash chromatography (SiO_2) with 8:1 dichloromethane/ethyl acetate afforded [G1]-Cl **(5a)** (8.37 g 8.38 mmol, 67%) as a light yellow solid: mp 115 °C, dec (CH_2Cl_2/EtOAc). ^{1}H NMR (400 MHz, $CDCl_3$) δ 1.91 (s, 6H), 1.95 (s, 6H), 2.33 (s, 6H), 3.63 (dd, $J = 4.0$, 11.6 Hz, 2H), 3.93 (dd, $J = 5.0$, 7.4 Hz, 2H), 4.44 (m, 2H), 5.81 (d, $J = 6.8$ Hz, 2H), 6.67 (d, $J = 9.2$ Hz, 2H), 7.03 (d, $J = 8.5$ Hz, 4H) 7.04 (d, $J = 8.5$ Hz, 4H), 7.14 (t, $J = 6.6$ Hz, 2H), 7.44 (d, $J = 7.6$ Hz, 2H), 7.45 (t, $J = 6.6$ Hz, 2H), 8.25 (d, $J = 7.6$ Hz, 2H), 8.30 (s, 2H), 12.00 (s, 2H); ^{13}C NMR (100 MHz, $CDCl_3$) 15.8, 21.1, 21.4, 52.8, 63.2, 74.2, 123.8, 125.3,125.8, 126.7, 127.7, 128.1, 132.7, 133.3, 137.3, 139.9, 148.6, 150.4, 161.5, 168.6, 170.8, 170.9 ppm; MS for $C_{49}H_{46}ClN_5O_{12}S_2$ (FAB) (M^+): Calcd 998.5; obsd 998.1. Anal. Calcd for $C_{49}H_{48}ClN_5O_{12}S_2$: C, 58.94; H, 4.85; N, 7.01. Found: C, 58.92; H, 4.81; N, 6.94.

4-Amino-2,6-bis((2-(1*S*,2*S*)-1-(4-methylthiophenyl)-1,3-propanediyl-bisacetate) Carbamoylphenyl)carbamoyl)pyridine (5c). [G1]-Cl **(5a)** (2.67 g, 2.67 mmol) and sodium azide (1.74 g, 26.7 mmol) were dissolved in 20 mL of DMF, and the solution was stirred at 45 °C for 48 h. The solvent was removed in vacuo, and the crude was taken up in CH_2Cl_2 (40 mL), washed with water (2 × 30 mL), dried over $MgSO_4$, and concentrated in vacuo. The crude azide (2.49 g, 2.49 mmol) was dissolved in 50 mL of THF−methanol (1:1), and the solution was degassed by sparging with argon for 10 min. Pd−C (10%, 0.249 g) was added, and the mixture was hydrogenated at 1 atm H_2 pressure for 48 h at room temperature. The catalyst was then removed by filtration through a pad of Celite with THF. The solvent was removed in vacuo, and the resultant solid was passed through a short plug of silica gel using THF affording [G1]-NH_2 **(5c)** as a white waxy solid (2.35 g, 2.40 mmol, 89%): mp 125 °C, dec (THF).^{1}H NMR (400 MHz, $CDCl_3$) δ 1.84 (s, 6H), 1.94 (s, 6H), 2.36 (s, 6H), 3.60 (dd, $J = 4.5$, 11.0 Hz, 1H), 3.96 (dd, $J = 4.8$, 11.0 Hz, 2H), 4.52 (m, 2H), 5.81 (d, $J = 7.0$ Hz, 2H), 6.68 (d, $J = 9.0$ Hz, 2H), 7.01 (d, $J = 8.3$ Hz, 4H) 7.05 (d, $J = 8.3$ Hz, 4H), 7.12 (t, $J = 7.6$ Hz, 2H), 7.40 (t, $J = 7.6$ Hz, 2H), 7.47 (d, $J = 6.4$ Hz, 2H), 7.48 (s, 2H), 8.18 (d, $J = 8.2$ Hz, 2H), 12.03 (s, 2H); ^{13}C NMR (100 MHz, $CDCl_3$) 14.8, 20.6, 20.9, 51.7, 62.67, 74.0, 108.9, 122.8, 124.5, 126.0, 126.5, 127.7, 129.2, 131.9, 134.1, 136.9, 138.6, 149.1, 158.0, 162.5, 168.3, 169.8, 170.4 ppm; MS for $C_{49}H_{50}N_6O_{12}S_2$ (FAB) (M^+): Calcd 979.1; obsd 979.4. Anal. Calcd for $C_{49}H_{50}N_6O_{12}S_2$: C, 60.11; H, 5.15; N, 8.58. Found: C, 59.90; H, 5.13; N, 8.61.

[G2]-Cl (6a). [G1]-NH_2 **(5c)** (200 mg, 0.204 mmol), DMAP (5 mg, 0.041 mmol), and triethylamine (0.030 mL, 0.216 mmol) were dissolved in CH_2Cl_2 (0.5 mL). 4-Chloro-pyridine-2,6-dicarbonyl chloride **(1)** (24 mg, 0.102 mmol) in 0.25 mL CH_2Cl_2 was then added dropwise via syringe to this mixture over 20 min. After stirring at room temperature for 16 h, the mixture was taken up in CH_2Cl_2 (2 mL). The CH_2Cl_2

solution was washed with 10% aqueous sulfuric acid (1 mL) and saturated aqueous sodium bicarbonate (1 mL) and then dried over $MgSO_4$ and concentrated in vacuo. Purification by flash chromatography (SiO_2) with 50:1 dichloromethane/methanol afforded [G2]-Cl **(6a)** (145 mg, 0.068 mmol, 67%) as a light yellow solid: mp 165 °C, dec (CH_2Cl_2/MeOH). ^{1}H NMR (400 MHz, DMSO-d_6) δ 1.85 (s, 12H), 1.93 (s, 12H), 2.40 (s, 12H), 3.62 (dd, J = 4.5, 11.0 Hz, 4H), 3.98 (dd, J = 4.5, 11.0 Hz, 4H), 4.48 (m, 4H), 5.67 (d, J = 8.0 Hz, 4H), 7.04 (d, J = 8.0 Hz, 8H), 7.11 (d, J = 8.0 Hz, 8H), 7.35 (t, J = 7.5, 4H), 7.62 (t, J = 7.6, 4H), 7.71 (d, J = 8.0 Hz, 4H), 8.29 (d, J = 8.0 Hz, 4H), 8.53 (s, 2H), 8.67 (d, J = 8.5 Hz, 4H), 9.03 (s, 4H), 11.77 (s, 2H), 12.17 (s, 4H); ^{13}C NMR (100 MHz, DMSO-d_6) 14.8, 20.6, 21.0, 51.8, 62.6, 74.0, 115.2, 124.8, 125.9, 126.2, 127.7, 129.2, 132.1, 134.1, 136.8, 138.6, 149.1, 150.0, 161.6, 162.4, 168.1, 169.8, 170.3 ppm; MS for $C_{105}H_{100}ClN_{13}O_{26}S_4$ (FAB) (M^+): Calcd 2123.7; obsd 2123.8. Anal. Calcd for $C_{105}H_{100}ClN_{13}O_{26}S_4$: C, 59.38; H, 4.75; N, 8.57. Found: C, 59.29; H, 4.87; N, 8.41.

[G2]-N_3 (6b). [G2]-Cl **(6a)** (717 mg, 0.338 mmol) and sodium azide (220 mg, 3.376 mmol) were dissolved in 3 mL of DMF, and the solution was stirred at 45 °C for 3 d. The solvent was removed in vacuo, and the crude was taken up in CH_2Cl_2 (10 mL), washed with water (2 × 5 mL), and then dried over $MgSO_4$ and concentrated in vacuo. Purification by flash chromatography (SiO_2) with 50:1 dichloromethane/methanol afforded [G2]-N_3 (0.419 g, 0.197 mmol, 58%) as a light yellow solid. ^{1}H NMR (500 MHz, DMSO-d_6) δ 1.85 (s, 12H), 1.93 (s, 12H), 2.40 (s, 12H), 3.62 (dd, J = 4.5, 11.0 Hz, 4H), 3.99 (dd, J = 4.5, 11.0 Hz, 4H), 4.49 (m, 4H), 5.68 (d, J = 8.0 Hz, 4H), 7.04 (d, J = 8.0 Hz, 8H), 7.11 (d, J = 8.0 Hz, 8H), 7.25 (t, J = 8.0, 4H), 7.61 (t, J = 8.0, 4H), 7.72(d, J = 8.0 Hz, 2H), 8.08 (s, 2H), 8.30 (d, J = 8.0 Hz, 4H), 8.66 (d, J = 8.5 Hz, 4H), 9.03 (s, 4H), 11.74 (s, 2H), 12.17 (s, 4H); ^{13}C NMR (125 MHz, DMSO-d_6) 14.8, 20.7, 21.0, 51.8, 62.6, 74.0, 115.2, 123.1, 124.8, 125.9, 126.2, 127.7, 129.3, 132.1, 134.1, 136.9, 138.6, 149.1, 150.0, 152.9, 161.7, 162.7, 162.8, 168.2, 169.8, 170.3 ppm; MS for $C_{105}H_{100}N_{16}O_{26}S_4$ (MALDI-TOF) (MH): Calcd 2128.3; obsd 2125.1.

[G2]-NH_2(6c). [G2]-N_3 **(6b)** (130 mg, 0.061 mmol) was dissolved in 5 mL of THF/methanol (1:1), and the solution was degassed by sparging with argon for 10 min. Pd−C (10%, 13 mg) was added, and the mixture was hydrogenated at 1 atm H_2 pressure for 48 h at room temperature. The catalyst was then removed by filtration through a pad of Celite with THF. The solvent was removed in vacuo and the residue purified by flash chromatography (SiO_2) going from 2 to 3% dichloromethane/methanol affording [G1]-NH_2 **(6c)** as a white waxy solid (92 mg, 0.044 mmol, 72%): mp 150 °C, dec (CH_2Cl_2/MeOH). ^{1}H NMR (400 MHz, $CDCl_3$) δ 1.87 (s, 12H), 1.95 (s, 12H), 2.43 (s, 12H), 3.65 (dd, J = 4.5, 11.0 Hz, 4H), 4.00 (dd, J = 4.5, 11.0 Hz, 4H), 4.50 (m, 4H), 5.70 (d, J = 7.0 Hz, 4H), 7.06 (d, J = 7.6 Hz, 8H), 7.14 (d, J = 8.0 Hz, 8H), 7.37 (t, J = 7.6, 4H), 7.63 (t, J = 7.6, 4H), 7.66 (s, 2H), 7.73 (d, J = 7.8 Hz, 4H), 8.31 (d, J = 8.0 Hz, 4H), 8.79 (d, J = 8.6 Hz, 4H), 9.05 (s, 4H), 11.62 (s, 2H), 12.18 (s, 4H); ^{13}C NMR (125 MHz, $CDCl_3$) 15.3, 21.2, 23.2, 52.3, 63.1, 74.5, 110.7, 115.7, 123.6, 124.8, 125.3, 126.4, 128.2, 129.8, 132.6, 134.6, 137.3, 139.1, 149.4, 149.9, 150.4, 157.7, 162.3, 164.7, 168.7, 170.8.3, 170.8 ppm; MS for $C_{105}H_{102}N_{14}O_{26}S_4$ (FAB) (MH): Calcd 2103; obsd 2103. Anal. Calcd for $C_{105}H_{102}N_{14}O_{26}S_4$: C, 59.93; H, 4.89; N, 9.32. Found: C, 59.74; H, 5.01; N, 9.10.

[G3]-Cl (7). [G2]-NH_2 **(7)** (106 mg, 0.050 mmol) was dissolved in a mixture of CH_2Cl_2 (0.5 mL) and pyridine (0.050 mL). Dry powdered molecular sieves (4 Å) (20 mg) were added, and the solution was stirred for 10 min. 4-Chloro-pyridine-2,6-dicarbonyl chloride **(1)** (6 mg, 0.025 mmol) in 0.1 mL CH_2Cl_2 was then added dropwise via syringe to this mixture over 5 min. After stirring at room temperature for 16 h, the mixture was taken up in CH_2Cl_2 (2 mL). The CH_2Cl_2 solution was washed with 10% aqueous sulfuric acid (1 mL) and saturated aqueous sodium bicarbonate (1 mL) and then dried over $MgSO_4$ and concentrated in vacuo. Purification by flash chromatography (SiO_2) with 50:1 dichloromethane/methanol afforded [G3]-Cl **(7)** (60 mg, 0.0137 mmol, 54%) as a light yellow solid: mp 195 °C, dec (CH_2Cl_2/MeOH). ^{1}H NMR (400 MHz, $CDCl_3$) δ 1.84 (s, 24H), 1.93 (s, 24H), 2.39 (s, 24H), 3.68(m, 8H), 3.99 (m, 8H), 7.49 (m, 8H), 5.69 (d, J = 6.7 Hz, 8H), 7.04 (d, J = 8.0 Hz, 16H), 7.12 (d, J = 8.0 Hz, 16H), 7.58 (t, J = 7.2 Hz, 8H), 7.70 (d, J = 7.2 Hz, 8H), 8.29 (d, J = 8.0 Hz, 8H), 8.52 (d, J = 8.0 Hz, 8H), 8.57 (s, 2H), 9.08 (s, 8H), 9.16 (s, 4H) 11.78 (m, 6H), 12.15 (s, 8H); ^{13}C NMR (100 MHz, $CDCl_3$) 16.6, 22.2, 22.5, 53.6, 64.3, 75.7, 117.0, 118.8, 124.8, 126.3, 127.8, 128.0, 129.3, 130.8, 133.6, 135.9, 138.6, 140.2, 150.9, 151.5, 151.7, 163.5, 165.0, 169.8, 171.3, 171.8 ppm; MS for $C_{217}H_{204}ClN_{29}O_{54}S_8$ (MALDI) (M + Na): Calcd 4397.1; obsd 4395.3. Anal. Calcd for $C_{217}H_{204}ClN_{29}O_{54}S_8$: C, 59.59; H, 4.70; N, 9.29. Found: C, 59.61; H, 4.82; N, 9.03.

[G0]-Control (8). [G0]-NH_2 **(4)** (300 mg, 0.72 mmol), picolinic acid (133 mg, 1.08 mmol), DMAP (9 mg, 0.07 mmol), and 1-(3-dimethylaminopropyl)-3-ethylcarbodiimide hydrochloride (EDCI) (207 mg, 1.08 mmol) were dissolved in 4 mL of DMF. After the mixture stirred at 50 °C for 12 h, the DMF was removed in vacuo, and the crude mixture was taken up in CH_2Cl_2 (10 mL), washed with water (2 × 10 mL), dried over $MgSO_4$, and concentrated in vacuo. Purification by flash chromatography (SiO_2) with 5:1 dichloromethane/ethyl acetate afforded [G0]-control **(8)** (235 mg, 0.45 mmol, 63%) as a white waxy solid: mp 193−194 °C (CH_2Cl_2/EtOAc). ^{1}H NMR (400 MHz, $CDCl_3$) δ 1.97 (s, 3H), 1.98 (s, 3H), 2.36 (s, 3H), 3.92 (dd, J = 5.0, 11.5 Hz, 1H), 4.12 (dd, J = 4.5, 11.5 Hz, 1H), 4.85 (m, 1H), 5.98 (d, J = 7.5 Hz, 1H), 6.44 (d, J = 9.0 Hz, 1H), 7.10 (t, J = 7.5 Hz, 1H), 7.14 (d, J = 8.4 Hz, 2H), 7.18 (obscured t, 1H), 7.23 (d, J = 8.4 Hz, 2H), 7.39 (d, 7.3 Hz, 2H), 7.49 (t, J = 8.0 Hz, 1H), 7.81 (t, J = 7.8 Hz, 1H), 8.21 (d, J = 7.0 Hz, 1H), 8.68 (bs, 1H), 8.76 (d, J = 8.3 Hz, 1H), 12.5 (s, 2H); ^{13}C NMR (100 MHz, $CDCl_3$) 15.8, 21.0, 21.4, 52.9, 63.6, 74.3, 122.2, 122.3, 123.0, 126.7, 126.9, 127.0, 127.8, 133.1, 133.2, 137.7, 139.2, 140.2, 149.0, 168.6, 170.9, 171.0 ppm; HRMS for $C_{27}H_{27}N_3O_6S$ (EI) (M^+): Calcd 521.1621; obsd 521.1628. Anal. Calcd for $C_{27}H_{27}N_3O_6S$: C, 62.17; H, 5.22; N, 8.06. Found: C, 62.41; H, 5.17; N, 8.04.

Acknowledgment. The authors thank Chris Hadad for help with the TDDFT-B3LYP calculations. Support for J.R during the course of this work from the Fullbright Commission and the University of Bonn is gratefully acknowledged. This work was supported by the National Science Foundation CAREER program (CHE 98-75458).

Supporting Information Available: Gaussian output for the TDDFT-B3LYP calculations and molecular orbital plots for the transitions described in Table 1 (PDF).This material is available free of charge via the Internet at http://pubs.acs.org.

JA001225C